Int. J. Electrochem. Sci., 16 **(2021)** 150541, doi: 10.20964/2021.01.35

International Journal of
ELECTROCHEMICAL
SCIENCE
www.electrochemsci.org

Characterization of the Electrochemical Properties of Nitrogen-Doped Graphene

Jinyan Song[1,*], *Suling Wang*[2], *Xiaolei Wang*[3], *Kai Wang*[4,*]

[1] School of Information Engineering, Dalian Ocean University, Dalian; 116023, China
[2] Department of Business Administration, Shandong Yingcai University, Ji'nan; 250104, China
[3] Qingdao Hisense Electronic Equipment Co., Ltd., Qingdao; 266071, China
[4] School of Electrical Engineering, Qingdao University, Qingdao; 266071, China
[*]E-mail: wkwj888@163.com and thesjyyan@163.com

Received: 6 May 2020 / *Accepted:* 3 November 2020 / *Published:* 30 November 2020

In recent years, graphene has attracted extensive attention in many fields. A nitrogen-doped graphene sheet was synthesized using a solid microwave-mediated method. An experimental electrode was thereafter prepared using nitrogen-doped graphene sheets (NGS), and the physical and electrochemical properties of nitrogen-doped graphene sheets were studied. A three-electrode supercapacitor test system with the experimental electrode also serving as one of the electrodes was built to conduct constant current charge/discharge, cyclic voltammetry, life span, and impedance spectrum tests on the experimental electrode. After 5000 cycles of charging/discharging at a current density of 0.5 A/g, the specific capacitance of the experimental electrode was 208.17 F/g with corresponding capacitance retention of 98.56%; when the current density was increased to 5 A/g, the specific capacitance of the experimental electrode after 5000 cycles of charging/discharging dropped to 157.31 F/g, indicating capacitance retention of 75.57%. The effective series resistance was approximately 0.32 Ω. Owing to the stable properties and high relative spatial surface area of NGS, ions have a good contact rate and charge exchange capacity between the electrode and the electrolyte interface, thereby ensuring a stable supercapacitor capacitance.

Keywords: Graphene oxide; Nitrogen-doped graphene; Melamine; Microwave; Energy storage

1. INTRODUCTION

In the concept of sustainable development, increasing attention is being paid to environmentally friendly energy sources and materials, such as supercapacitors [1-5], lithium batteries [6-11], nanogenerators [12-15], and other energy storage [16-20]. The main advantage of a supercapacitor is its ability to store electric energy, which makes it suitable for use as an active

component in electronic circuits. Electrochemical capacitors with high energy storage capacity can be used in the storage of electric energy generated by solar photovoltaic systems. The development of high-performance energy storage devices has attracted worldwide attention [21-25]. Although electrochemical capacitor technology development has been slow, many products and applications have been developed. Existing research on the cycle life of energy storage devices and the materials used in them has improved the performance of the devices. However, with the rapid development of the Internet of Things and sensor networks, the performance requirements of wearable sensors are becoming increasingly high. The power requirements of many energy storage components are yet to be met. The biomechanical energy generated by the human body is lost to the surrounding environment [26-29]. If converted to electrical energy, this energy can be used to power wearable sensors and, therefore, has high potential for development [30-33]. However, biomechanical energy of the human body has to be collected effectively. To this end, graphene is a type of carbon material that has undergone rapid development in recent years. Because it consists of only a single layer of graphite atoms, graphene has a large relative surface area and stable physical and chemical properties while being safe for environmental applications and human use [34-37]. Graphene is an excellent material for use in supercapacitor electrodes. At present, graphene production required the reduction of graphite oxide; natural flake graphite is first oxidized using Hummers method to obtain graphite oxide [38-41]. The oxygen-containing functional group in the graphite oxide is thereafter stripped by a reduction method to obtain a discrete graphite sheet, called grapheme [42-45].

In practical applications, the strong interlayer van der Waals forces, mutual attraction, and agglomeration between the sheets cause the relative surface area of graphene to decrease, and its resistivity to increase [46-50]. In addition, the agglomeration phenomenon of graphene worsens as the charge/discharge time increases, especially at high working currents [51-53]. Therefore, research in the field has focused on suppressing agglomeration in graphene [54-56]. At present, nitrogen doping is used to suppress agglomeration in graphene because nitrogen atoms, being similar to carbon atoms in volume and mass, can exist in the graphene lattice structure [57-59].

After the nitrogen atoms are doped into the graphene, the original uniform layered structure of graphene is disturbed as random defects begin to develop, thereby considerably reducing the interlayer van der Waals forces, and satisfactorily suppressing the agglomeration phenomenon [60]. Praveen et al. used nitrogen doping of graphene at a high temperature, and electrochemically tested the prepared nitrogen-doped graphene (with a nitrogen content of 4.5%). After 500 cycles, the material had a specific capacitance of 190 F/g at a current density of 1 A/g, a capacity attenuation of 7.8%, and an equivalent series resistance of 0.17 Ω. Therefore, the material can be used to prepare small-capacity supercapacitors [61-63]. The prepared material had a stable physical structure, excellent electrical conductivity, high specific capacitance, and high cycle stability [64-66].

The aim of this study was to develop a new method for preparing nitrogen-doped graphene electrode materials using natural flake graphite as raw material, melamine as a functional agent, and nitrogen as a dopant. The nitrogen atoms in the melamine were doped into the graphite sheet lattice structure using the high instantaneous heat generated by microwaves. The method does not use ammonia gas, which is a highly toxic nitrogen dopant. The method will be excellent for preparing nitrogen-doped graphene materials because of the low cost and eco-friendliness of the raw materials

used and the convenience and safety of the adopted method.

2. EXPERIMENTAL

2.1. Preparation of the graphite oxide

Graphite oxide (GO) was prepared using modified Hummers method [67-69]. First, 130 mL of concentrated sulfuric acid (mass fraction: 98%, Beijing Chemical Reagents Co. Ltd.) and 5 g of natural flake graphite (Beijing Chemical Reagents Co. Ltd.) were added to a 1 L beaker, and the resulting mixture was stirred for 2 h in an ice bath. Secondly, 15 g of potassium permanganate (Zhengzhou No. 3 Chemical Reagent Factory) was slowly added to the mixture, which was stirred in the ice bath for another 2 h. The mixture was thereafter stirred in a constant-temperature water bath for 35 h to facilitate further oxidation. Finally, 230 mL of ionized water was added to the beaker, and the mixture was slowly heated to 98 °C and cooled to room temperature of 20°C for 30 min. Subsequently, 400 mL of deionized water was added to the mixture and the solution was centrifuged several times. GO suspension was obtained when the solution became completely neutral.

2.2. Preparation of nitrogen-doped graphene

A solution was prepared by adding 3.26 g of melamine (Xinji JiuYuan Chemical Reagent Co. Ltd) to 100 mL of deionized water, and the resulting aqueous solution was stirred for 2.5 h at 95 °C. The GO suspension was diluted to 1 mg mL^{-1}, and 100 mL of it and 100 mL of the melamine aqueous solution were mixed in a flask and refluxed for 10 h at 97 °C. The resulting precipitate was freeze-dried to prepare solid functionalized graphene nanosheets (FGS). Finally, the FGS were placed in a quartz reactor (23 L, 315 mm × 349 mm × 207 mm) and treated in a microwave oven (Panasonic, NN-GT353M) for 90 s in an atmosphere of argon to obtain nitrogen-doped graphene.

2.3. Preparation of the experimental electrode

Nitrogen-doped graphene was repeatedly washed with deionized water, centrifuged until the solution was neutral, dried in an argon atmosphere for 12 h, and finally ground for 2 h using a planetary ball mill (QM-QX04, Nanjing University Instrument Factory). The ground nitrogen-doped graphene, which is called graphite, and polytetrafluorethylene were uniformly mixed at a mass ratio of 8:1:1, and ground for 1 h using a natural agate mortar. An appropriate quantity of absolute ethanol was then added to the slurry. The slurry was then ultrasonically treated for 1 h. Thereafter, an appropriate quantity of polytetrafluorethylene was added as a binder to the nitrogen-doped graphene, the coating was reapplied, and graphene was dried to prepare the electrode. The prepared electrode was cut into a 1 × 1 cm square and was weighed using an electronic balance. The electrode was then pressed using a roll mill at a pressure of 12 MPa onto a foamed nickel mesh current collector to prepare the experimental electrode [30].

2.4. Synthesis scheme of nitrogen-doped graphene

Fig. 1 shows the synthetic route used to prepare nitrogen-doped graphene. First, the amino functional group in melamine and the oxygen-containing functional group on the surface of GO underwent ring-opening reaction, and the melamine molecules were grafted onto GO to form functionalized graphite on the surface. Because many incompletely oxidized conjugated regions were present, the temperature of the region was sharply increased using microwave irradiation to strip the oxygen-containing functional groups. Consequently, the melamine functional groups were decomposed, and nitrogen atoms were doped into the graphene lattice. Table 1 compares the synthesis schemes of various nitrogen-doped graphene.

Table 1. Comparison of synthetic schemes of various nitrogen-doped graphene.

Electrode materials	Preparation of the graphite oxide	Preparation of nitrogen-doped graphene	Reference
NGS	modified Hummer's method	microwave irradiation	This work
NGS-HMT	modified Hummer's method	hydrothermal process	61
NG	modified Hummer's method	annealed in the atmosphere of ammonia	64
aNG	modified Hummer's method	thermal annealing method	65
NRGO-H	modified Hummer's method	hydrothermal reduction	66
3D graphene	modified Hummer's method	solid-state pyrolysis	69

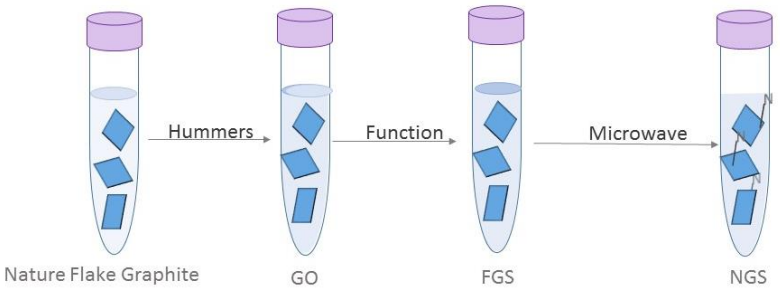

Figure 1. Synthetic scheme of NGS (Graphene Oxides (GO), Functionalized Graphene Sheets (FGS), Nitrogen-doped Graphene Sheets (NGS))

3. RESULTS AND ANALYSIS

3.1. Characterization of the physical and chemical properties of graphene electrode materials

3.1.1. Analysis of electron microscope surface topography

Fig. 2 displays the scanning electron microscope (SEM) and transmission electron microscope (TEM) images of GO, FGS, and NGS. Because of the intense van der Waals interactions between the adjacent layers of the GO sheets, the images of the Go sheets are plotted together in Fig. 2(a). Because of functionalization, FGS layers are spread stochastically, and the corresponding slices become more apparent to electrons than to the GO layers as displayed by the flaky slices of FGS depicted in Fig. 2 (b). Thus, the van der Waals interactions between the adjacent layers of GO sheets can be effectively reduced by functionalization. NGS has a rugose and lapped surface as displayed in Fig. 2 (c). The folds on the outside layer of NGS are evenly distributed, resulting in a large superficial area. The synthesis of graphene using microwave radiation and functionalized GO is, therefore, feasible. A representative image of NGS is shown in Fig. 2 (d). High specific surface area nanosheets have joined together to form a multideck structure as the nitrogen atoms enter the lattices of graphene. NGS can be used in power storage devices to improve their performance.

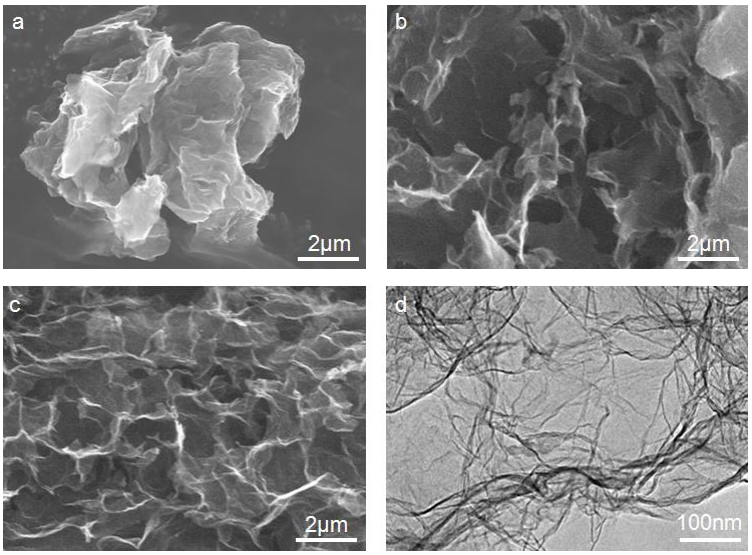

Figure 2. (a) SEM image of GO; (b) SEM image of FGS; (c) SEM image of NGS; and (d) TEM image of NGS.

3.1.2. Analysis of the BET space volumes and XRD

The nitrogen adsorption isotherm and BJH aperture distribution of NGS at 77 K are shown in Fig.3 (a). As the figure displays, NGS has a type IV isotherm. The superficial area of the NGS is 446 m^2/g, which is smaller than its theoretical relative surface area because of the overlapping of the graphene sheets. The adsorption curve of NGS displays a hysteresis effect, proving that its internal structure is porous. The inset in Fig. 3 (a) displays the pore size distribution of NGS, which shows a

peak in pore volume at a pore width of 20 nm, mainly in the range of 5–40 nm, beyond which the pores are exceeded. The number has dropped dramatically. At 0.98 P_0, the total pore volume is approximately 1.62 cm^3/g, which indicates that the electrochemical performance of the material is acceptable for use in energy storage devices.

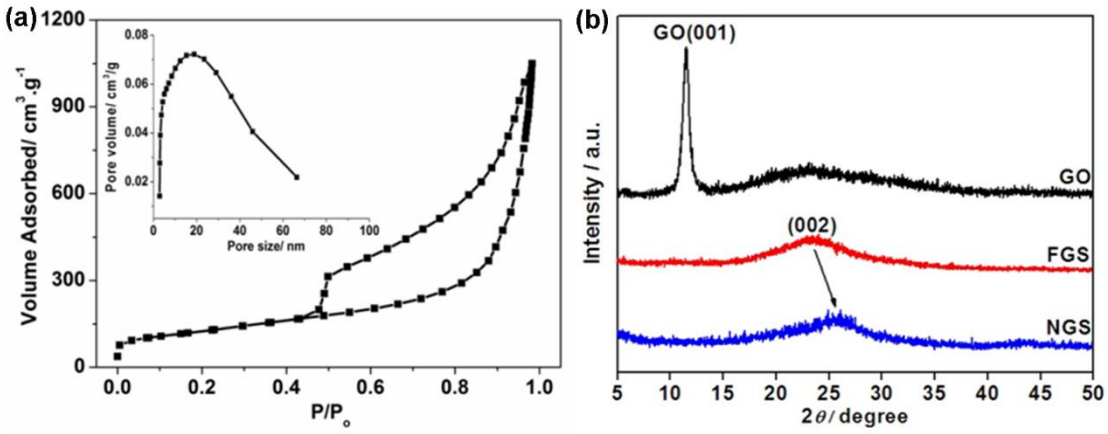

Figure 3. (a) The pore size distribution (b) XRD patterns of GO, FGS and NGS

The X-ray diffraction (XRD) patterns of GO, FGS, and NGS are shown in Fig. 3 (b). The diffraction maximum of GO (001) occurs at 2θ =11.39°. Thus, the van der Waals interactions between adjacent layers of GO are substantially weaker than those of graphite. The (001) diffraction maximum is absent in the FGS spectrum because of functionalization, revealing that the van der Waals interactions between adjacent FGS layers have been further reduced by the transplanted melamine molecules, preventing the FGS layers from getting restacked. The multilayer characteristics of the graphene sheets can be observed by analyzing the wide peak in the 20° to 30° 2θ range. The NGS peak is broader because of the effect of microwaves, indicating that the space between the layers has become narrower. Melamine is decomposed under the rapid calefaction produced by microwaves, which causes the transfer of the corresponding peaks.

3.2. Electrical performance testing of the Supercapacitor

A three-electrode supercapacitor test system, consisting of the experimental electrode and two other electrodes, was built for conducting constant current charge/discharge, cyclic voltammetry, life span, and impedance spectrum tests using a CHI660A electrochemical workstation (Shanghai Chenhua Instrument Co., Ltd.). In the three-electrode system, a platinum electrode was used as the auxiliary electrode, a saturated calomel electrode as the reference electrode. The electrolyte used was 3 mol/L sodium hydroxide aqueous solution.

3.2.1. Cyclic voltammetry test

In general, the power density obtained by using electrochemical capacitors and batteries will increase as the temperature increases. Fig. 4 shows the cyclic voltammetry curve of a nitrogen-doped

graphene experimental electrode at scan speeds of 5, 10, and 20 mV/s. All three curves have almost rectangular shapes, indicating that the charge absorption and release of the experimental electrode during its charging and discharging are based on the double electric layer principle. However, the oxidation-reduction reaction is less affected, and the curve area is larger, which proves the experiment. The specific capacitance of the electrode was higher.

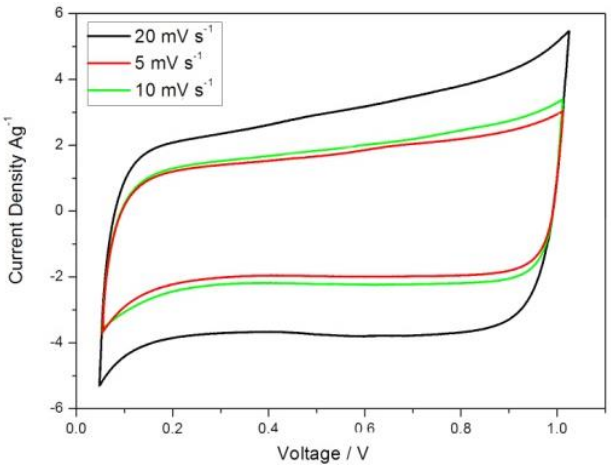

Figure 4. The cyclic voltammetric measurement under different scan rate (5, 10 and 20 mV/s) of Nitrogen-doped Graphene Sheets (NGS) electrode (the different line segments show scan rate)

3.2.2. Constant current charge / discharge tests

Fig. 5 displays the constant current charge/discharge curves of the NGS electrode at current densities of 0.5 A/g, 1 A/g, and 5 A/g. The specific capacitance of the electrode at a current density of 0.5 A/g calculated using the discharge curve is 208.17 F/g. Even when the current density is increased to 5 A/g, the specific capacitance drops only to 157.31 F/g. The percentage retention of the specific capacitance is 75.57%, which proves that the experimental electrode can maintain high capacitance even with high charge and discharge currents.

Table 2. Comparison of specific capacitance of nitrogen-doped graphene synthesized in different literatures at low and high current densities.

Electrode materials	Specific capacitance/F g^{-1} (at low current density)	Specific capacitance/F g^{-1} (at high current density)	Reference
NGS	208.17 F g^{-1} (at 0.5 A g^{-1})	157.31 F g^{-1} (at 5 A g^{-1})	This work
NGS-HMT	161 F g^{-1} (at 0.5 A g^{-1})	141 F g^{-1} (at 4 A g^{-1})	61
NGF	117.4 F g^{-1} (at 0.5 A g^{-1})	88.1 F g^{-1} (at 4 A g^{-1})	63
NRGO-H	332 F g^{-1} (at 0.5 A g^{-1})	206 F g^{-1} (at 5 A g^{-1})	66
3D graphene	175 F g^{-1} (at 0.5 A g^{-1})	75 F g^{-1} (at 5 A g^{-1})	69

Furthermore, the charge/discharge curves of the electrode are smooth and symmetrical, proving

that there will be no space collapse inside the electrode during its charging and discharging and that its cycle stability is high. Table 2 compares the specific capacitance of nitrogen-doped graphene synthesized in different literatures at low current density and high current density.

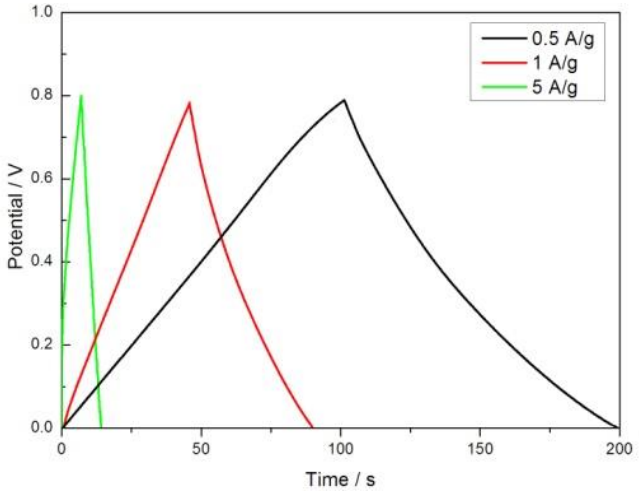

Figure 5. Constant current charge and discharge curve of nitrogen-doped graphene Nitrogen-doped Graphene Sheets (NGS) electrode at the current density of 0.5, 1 and 5 A/g (the different line segments show current density)

3.2.3. Life span test

Fig. 6 shows the variation of the specific capacitance of the NGS experimental electrode with the charge/discharge current. At the end of the 5000th charge/discharge cycle, the specific capacitances of the electrode were 157.31 F/g and 138.31 F/g when the current densities were 5 A/g and 40 A/g, respectively, which correspond to 75.59% and 66.44% of their initial values, respectively. When the current density is between 0 – 5 A, the experimental electrode capacitance decreases sharply. The decay rate of the specific capacitance is significant even in the 5 – 10 A interval. When the current density is beyond 10 A/g, the rate of decrease of the specific capacitance of the electrode is reduced, thereby stabilizing the electrode.

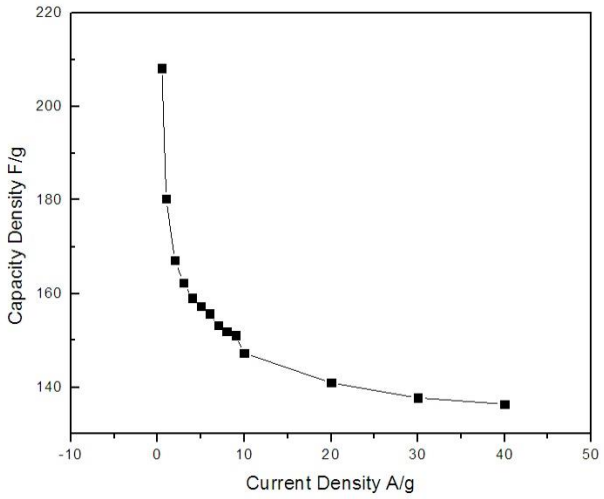

Figure 6. The specific capacitances of the Nitrogen-doped Graphene Sheets (NGS) electrode at different current densities

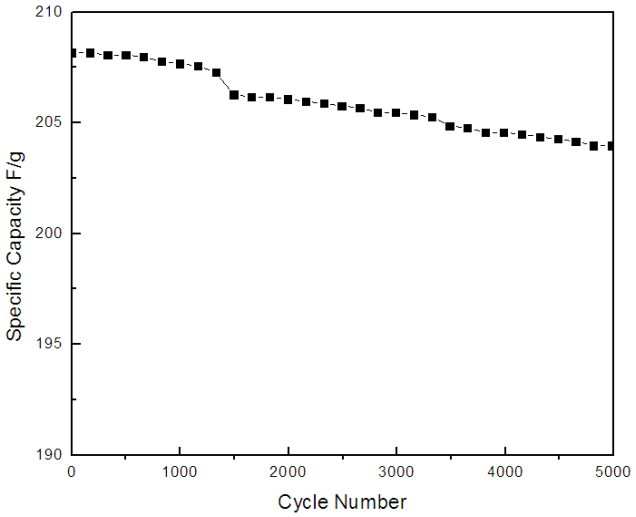

Figure 7. The cycling life of the Nitrogen-doped Graphene Sheets (NGS) electrode under 5000 cycles of charge and discharge experiments with a current density of 0.5 A/g

Fig. 7 shows the cycle stability of the experimental electrode, a parameter important for testing the performance of supercapacitor electrode material, after 5000 charge/discharge cycles at a current density of 0.5 A/g. The specific capacitance of the electrode after the 5000th cycle is approximately 98.56% of its initial value, proving that the internal structure of nitrogen-doped graphene remains stable during its charge/discharge and that it has no internal space.

3.2.4. Impedance spectrum test

Fig. 8 shows the impedance spectrum of the experimental electrode, which is slightly curved in the high-frequency region. The approximate equivalent series resistance of the electrode is 0.32 Ω. In

the low-frequency region, the curve is almost linear, indicating the capacitor characteristics of the electrode.

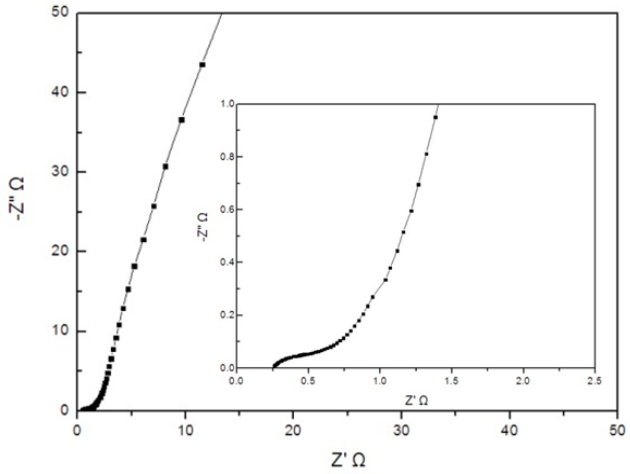

Figure 8. The impedance characteristics of the Nitrogen-doped Graphene Sheets (NGS) electrode

Table 3 summarizes the cyclic stability and equivalent series resistance of electrode materials reported previous researchers. It can be seen from the table that NGS has higher cyclic stability and lower equivalent series resistance.

Table 2. Comparison of cyclic stability and equivalent series resistance of electrode materials reported by previous researchers.

Electrode materials	Cycle stability (Specific capacitance retention rate)	Approximate equivalent series resistance	Reference
NGS	98.56% (after 5000 cycles)	0.32 Ω	This work
NGS-HMT	98.10% (after 5000 cycles)	3.70 Ω	61
NDG	97.00% (after 5000 cycles)	3.80 Ω	62
NG	90.10% (after 5000 cycles)	0.05 Ω	64
N-rGO/Fe_2O_3	95.97% (after 5000 cycles)	0.31 Ω	67
HNG/Co_3O_4	84.50% (after 5000 cycles)	1.20 Ω	68

4. CONCLUSIONS

This study explored an efficient method for NGS production using GO that was functionalized using melamine and microwave radiation. The prepared NGS displayed a highly porous structure with a BET surface area of 446 m^2/g. The experimental electrode had a high current tolerance and a long cycle life. The specific capacitance of the electrode was high at 208.17 F/g after 5000 cycles of charging/ discharging at a current density of 0.5 A/g. When the current density was increased to 5 A/g, the specific capacitance dropped to 157.31 F/g after 5000 charging/discharging cycles, indicating a capacitance retention of 75.57%. The capacitance retention of the experimental electrode after 5000 charging/ discharging cycles at a current density of 0.5 A/g was 98.56%. The effective series resistance of the electrode was approximately 0.32 Ω. Compared with other electrode materials, nitrogen-doped

graphene electrode material maintain a stable internal space morphology during the charge–discharge cycles. Owing to the stable physicochemical properties of NGS and its high relative spatial surface area, ions have a good contact rate and charge exchange capacity between the electrode and the electrolyte interface to ensure a stable supercapacitor capacitance.

ACKNOWLEDGMENTS
This work was supported by Liaoning Province Natural Fund Guidance Plan (20180550573) -Hybrid energy storage system and performance degradation mechanism of the underwater robot research, the Scientific Research Development Plan of Shandong Higher Education Institutions (No. J18KA316), Development Plan of Shandong Province (No. 2019GGX104019).

References

1. G.T. Xia, C. Li, K. Wang and L.W. Li, *Sci. Adv. Mater.*, 11 (2019) 1079-1086.
2. L. Guang, H. H, L.Q. Li and et al, *ACS Nano*, 14 (2020) 6222-6231.
3. H.X. Liu, L. Zhao, Y.T. Zhou, J.Y. Song, K. Wang and L.W. Li, *Sci. Adv. Mater.*, 11 (2019) 1072-1078.
4. K. Wang, L.W. Li, T.Z. Zhang and Z.F. Liu, *Energy*, 70 (2014) 612-617.
5. K. Wang, L.W. Li and H. Zhang, *Int. J. Electrochem. Sci.*, 8 (2013) 5036-5041.
6. X. Luo, F.L. Zhang, Q. Li, Q.T. Xia, Z.H. Li, X.K. Li, W.N. Ye, S.D. Li and C. Ge, *J. Phys. Condens. Matter*, 32 (2020) 334001.
7. F. Zhang, X. Teng, W. Shi, Y. Song, J. Zhang, X. Wang, H. Li, Q. Li, S. Li and H. Hu, *Appl. Surf. Sci.*, 52 (2020) 146910.
8. Q.C. Sun, X. Luo, Q.T. Xia, Y.F. Guo, J. Su, Q. Li and G. X, *J. Magn. Magn. Mater.*, 499 (2020) 166317.
9. S.T. Fan, J. Zhang and X. L. Teng, *J. Electrochem. Soc.*, 166 (2019) A3072-A3078.
10. Y.Z. Qin, Q. Li and J. Xu, *Electrochim. Acta*, 224 (2017) 90-95.
11. Q. Xue, Y.H. Yang, Z.W. Gao, *Appl. Phys. Lett.*, 109 (2016) 192407.
12. X.X. Wang, W.Z. Song, M.H. You, J. Zhang, M. Yu, Z.Y. Fan, S. Ramakrishna and Y.Z. Long, *ACS Nano*, 12 (2018) 8588-8596.
13. X. Feng, Y. Zhang, L. Kang, L.C. Wang, C.X. Duan, K. Yin, J.B. Pang and K. Wang, *Front. Chem. Sci. Eng.*, (2020) DOI: 10.1007/s11705-020-1956-3.
14. C.Y. Bu, F.J. Li, K. Yin, J.B. Pang, L.C. Wang and K. Wang, *ACS Appl. Electron. Mater.*, 2 (2020) 863-878.
15. G.T. Xia, Y.N. Huang, F.J. Li, L.C. Wang, J.B. Pang, L.W. Li and K. Wang, *Front. Chem. Sci. Eng.*, 14 (2020) 1039-1051.
16. S.F. Tang, Z.T. Wang, D.L. Yuan, Y.T. Zhang, J.B. Qi, Y.D. Rao, G. Lu, B. Li, K. Wang and K. Yin, *Int. J. Electrochem. Sci.*, 15 (2020) 2470-2480.
17. L.C. Wang, R. Yan, F. Bai, T.K. Saha and K. Wang, *IEEE Trans. Sustain. Energy*, 11(2020) 2687-2697.
18. D.L. Yuan, M.T. Sun, M.Z. Zhao, S.F. Tang, J.B. Qi, X.Y. Zhang, K. Wang, B. Li, *Int. J. Electrochem. Sci.*, 15 (2020) 8761-8770.
19. S.F. Tang, J.C. Tang, D.L. Yuan, Z.T. Wang, Y.T. Zhang and Y.D. Rao, *RSC Adv.*, 10 (2020) 17627-17634.
20. Y.T. Zhou, Y.N. Huang, J.B. Pang and K. Wang, *J. Power Sources*, 440 (2019) 227149.
21. K. Wang, L.W. Li, Y. Lan, P. Dong and G.T. Xia, *Math. Probl. Eng.*, 2019 (2019) 2614327.
22. H.L. Du, C.Y. Ma, W.X. Ma and H.T. Wang, Process *Appl. Ceram.*, 12 (2018) 303-312.
23. M. Arshad, H.L. Du, M.S. Javed, A. Maqsood, I. Ashraf, S. Hussain, W.L. Ma and H.P. Ran,

Ceram. Int., 46 (2019) 2238-2246.
24. Q.L. Cheng, J.B. Pang, D.H. Sun, J.G. Wang, S. Zhang, F. Liu, Y.K. Chen, R.Q. Yang, N. Liang, X.H. Lu, Y.C. Ji and J. Wang, *Infomat*, 2 (2020) 656-697.
25. J.R. Wu, K. Yin, M. Li, Z.P. Wu, S. Xiao, H. Wang, J.A. Duan and J. He, *Nanoscale*, 12 (2020) 4077-4084.
26. C. Duan, Y. Yu, J. Xiao, X. Zhang, L. Li, P. Yang, J. Wu and H. Xi, *Sci. China Mater.*, 63 (2020) 667-685.
27. K. Wang, X. Feng, J.B. Pang, J. Ren, C.X. Duan, L.W. Li, *Int. J. Electrochem. Sci*, 15 (2020) 9499-9516.
28. Y.T. Zhou, Y.N. Wang, K. Wang, L. Kang, F. Peng, L.C. Wang and J.B. Pang, *Appl. Energy,* 260 (2020) 114169.
29. Y. Li, X. Zhou, W. Qi, H. Xie, K. Yin, Y. Tong, J. He, S. Gong and Z. Li, *Chem. Eng. J.*, 383 (2020) 123086.
30. K. Wang, S.Z. Zhou, Y.T. Zhou, J. Ren, L. W. Li and Y. Lan, *Int. J. Electrochem. Sci.*, 13 (2018) 10766-10773.
31. K. Wang, C. Li and B.C. Ji, *J. Mater. Eng. Perform.*, 23 (2014) 588-592.
32. M. Zhang, K. Wang and Y. Zhou, *Complexity*, 2020 (2020) 8231243.
33. C. Duan, Y. Yu, J. Xiao, Y. Li, P. Yang, F. Hu and H. Xi, *Green Energy Environ.*, (2020), DOI: 10.1016/j.gee.2020.04.006.
34. K. Wang, L.W. Li, H.X. Yin, T.Z. Zhang and W.B. Wan, *PloS One*, 10 (2015) e0138672.
35. C.Z. Zhu, Y.Z. Ma and Q.K. Bu, *Int. J. Electrochem. Sci.*, 13 (2018) 10207-10216.
36. Z.Q. Dai, K. Wang and L.W. Li, *Int. J. Electrochem. Sci.*, 8 (2013) 9384-9389.
37. J.R. Wu, K. Yin, M. Li, S. Xiao, Z.P. Wu, K. Wang and J.A. Duan, *Colloids Surf. A Physicochem. Eng. Asp.*, (2020) 125030.
38. W. Gao, L.B. Alemany, L.J. Ci and P.M. Ajayan, *Nature Chem*., 1 (2009) 403.
39. T. Pichler, *Nature Mater.*, 6 (2007) 332.
40. K. Wang, L.W. Li and H. Zhang, *Int. J. Electrochem. Sci.*, 8 (2013) 4785-4791.
41. K. Wang, J.B. Pang, L.W. Li, S.Z. Zhou, Y.H. Li and T.Z. Zhang, *Front. Chem. Sci. Eng.*, 12 (2018) 376-382.
42. K. Wang, W.L. Wang, L.C. Wang, L.W. Li, Energies, 13 (2020), 5297.
43. K. Wang, B. Ji and M. Han, *Chinese J. Inorg. Chem.*, 29 (2013) 2105-2109.
44. C.G. Liu, Z.N. Yu and D. Neff, A. Zhamu, B.Z. Jang, *Nano Lett.*, 10 (2010) 4863.
45. M. Janani, P. Srikrishnarka, S.V. Nair and A.S. Nair, *J. Mater. Chem. A*, 3 (2015) 17914.
46. K. Wang, L.W. Li and T.Z. Zhang, *Int. J. Electrochem. Sci.*, 8 (2013) 6252-6257.
47. D. Lin, Y. Liu, Z. Liang, H.W. Lee, J. Sun, H. Wang, K. Yan, J. Xie and Y. Cui, *Nat. Nanotechnol.*, 11 (2016) 626.
48. K. Wang, L.W. Li and T.Z. Zhang, *Int. J. Electrochem. Sci.*, 8 (2013) 6900-6904.
49. H. Hu and M.B. Wu, *J. Mater. Chem. A*, 8 (2020) 7066-7082.
50. Q. Li, H.S. Li, Q.T. Xia, Z.Q. Hu, Y. Zhu, S.S. Yan, C. Ge, Q.H. Zhang, X.X. Wang, X.T. Shang, S.T. Fan, Y.Z. Long, L. Gu, G.X. Miao, G.H. Yu, J.S. Moodera, *Nat. Mater.*, 2020, DOI:10.1038/s41563-020-0756-y.
51. K. Wang, L.W. Li and X.Z. Wu, *Int. J. Electrochem. Sci.*, 8 (2013) 6763-6766.
52. H. Hu, Q. Li, L.Q. Li, X.L. Teng, Z.X. Feng, Y.L. Zhang, M.B. Wu and J.S. Qiu, *Matter*, 3 (2020) 95-126.
53. K. Wang, L.W. Li and X.Z. Wu, *Int. J. Electrochem. Sci.*, 8 (2013) 6574-6578.
54. W.Z. Huang, Q. Yang, X.D. Ye and F.Z. Kong, *Mater. Rev.*, 7 (2012) 26.
55. Y.P. Fu, H.F. Wang, G.D. Tian, Z.W. Li and H.S. Hu, *J Intell. Manuf.*, 30 (2019) 2257-2272.
56. K. Wang, L.W. Li, W. Xue, S.Z. Zhou, Y. Lan, H.W. Zhang and Z.Q. Sui, *Int J. Electrochem. Sci.*, 12 (2017) 8306-8314.
57. S.F. Tang, M.Z. Zhao, D.L. Yuan, X. Li, X.Y. Zhang, Z.B. Wang, T.F. Jiao, K. Wang., *Sep. Purif.*

Technol., 255 (2021) 117690.
58. K. Wang, C.L. Liu, L.C. Wang, J.Y. Song, C.X. Duan, L.W. Li, *Complexity*, 2020 (2021) 1-18.
59. Y.P. Fu, Y. Wang, D. Wu, H.F. Wang, *Transp. Res. Pt. A-Policy Pract.*, 138 (2020) 172-186.
60. W.L. Wang, Y.H. Li, L.W. Li, L.C. Wang, K. Wang, *Int. J. Electrochem. Sci.*, 15(2020), DOI: 10.20964/2020.12.49
61. J.W. Lee, J.M. Ko, and J.D. Kim, *Electrochim. Acta*, 85 (2012) 459-466.
62. V. Sahu, S. Grover, B. Tulachan, M. Sharma, G. Srivastava, M. Roy, M. Saxena, N. Sethy, K. Bhargava, D. Philip, H. Kim, G. Singh, S.K. Singh, M. Das and H. Kim. *Electrochim. Acta*, 160 (2015) 244-253.
63. X. Xiao, Y.X. Zeng, H.B. Feng, K.Q. Xu, G.B. Zhong, S.J. Wu, C. Wang, W. Zhao, W. Su, Z.F. Wei and X.H. Lu, *ChemNanoMat*, 5 (2019) 152-157.
64. F. Jiang, J.X. Zhang, N. Li, C. Liu, Y.Q. Zhou, X.L. Yu, L.D. Sun, Y.P. Song, S.D. Zhang and Z.Y. Wang, *J. Chem. Technol. Biotechnol.*, 94 (2019) 3530-3537.
65. B. Zheng, T.W. Chen, F.N. Xiao, W.J. Bao and X.H. Xia, *J. Solid State Electrochem.*, 17 (2013) 1809-1814.
66. P. Bharathidasan, M.B. Idris, D.W. Kim, S.R. Sivakkumar and S. Devaraj, *FlatChem*, 11 (2018) 24-31.
67. H.D. Liu, J.L. Zhang, D.D. Xu, L.H. Huang, S.Z. Tan and W.J. Mai, *J. Solid State Electrochem.*, 19 (2015) 135-144.
68. X. Liu, Z. Wu, and Y. Yin, *Synth. Met.*, 223 (2017) 145-152.
69. D. He, W. Wang, Y. Fu, R. Zhao, W. Xue and W. Hu, *Composites, Part A*, 91 (2016) 140-144.